

# Fermi-liquid instability of $\text{CeRh}_2\text{Si}_2$ near a pressure-induced quantum phase transition

Masashi Ohashi and Gendo Oomi

*Department of Physics, Kyushu University, Fukuoka 812-8581, Japan*

Sadayoshi Koiwai

*Department of Physics, Saitama University, Saitama 338-0825, Japan*

Masato Hedo and Yoshiya Uwatoko

*Institute of Solid State Physics, University of Tokyo, Kashiwa 277-8581, Japan*

(Received 19 March 2003; published 21 October 2003)

The electrical resistivity of single crystalline  $\text{CeRh}_2\text{Si}_2$  has been measured at high pressure up to 8 GPa, and low temperature down to 2.0 K for the current along the  $a$  and  $c$  axes. Two magnetic phase transitions  $T_{N1} = 35$  K and  $T_{N2} = 24$  K at ambient pressure were observed as a function of pressure. It is found that both transitions  $T_{N1}$  and  $T_{N2}$  are suppressed by applying pressure and disappear near the critical pressure at  $P_{C1} \sim 1.0$  GPa and  $P_{C2} \sim 0.6$  GPa, respectively. The transition for  $T_{N1}$  is second order and the one for  $T_{N2}$  is first order. The resistivity shows  $T^2$  dependence at low temperature in a wide pressure range from ambient pressure up to 8 GPa, indicating that a Fermi liquid state still exists near  $P_{C1}$  and  $P_{C2}$ . According to the comparison between the coefficient of  $T^2$  term and the Sommerfeld coefficient  $\gamma$ , however, it is suggested that the enhancement of many-body dynamical effect occurs near the critical pressure  $P_{C1} \sim 1.0$  GPa. These results are discussed on the basis of the pressure-induced quantum phase transition.

DOI: 10.1103/PhysRevB.68.144428

PACS number(s): 75.20.Hr, 73.43.Nq, 74.62.Fj

## I. INTRODUCTION

A quantum phase transition (QPT) occurs at 0 K in a highly correlated electron system due to variation of nonthermal control parameters which gives rise to fundamental change in the ground state. The typical parameters to tune QPT are the chemical composition, pressure, or magnetic field. While phase transitions in classical models are driven only by thermal fluctuations as classical systems usually freeze into a fluctuationless ground state at  $T=0$ , quantum systems have fluctuations driven by the Heisenberg uncertainty principle even in the ground state. The  $T>0$  region in the vicinity of a quantum critical point (QCP), however, offers a fascinating interplay of effects driven by quantum and thermal fluctuations. This means that working outward from QCP is a powerful way of understanding and describing the thermodynamic and dynamic properties of numerous systems in which QPT occurs. Indeed, unusual electronic and magnetic behaviors can arise near nonzero temperature.<sup>1,2</sup> If the magnetic ordering temperature in a heavy fermion (HF) system is suppressed to absolute zero by tuning the control parameter, magnetic fluctuations lead to strong enhancement of the quasiparticle scattering rate and potentially to a breakdown of the Fermi liquid (FL) description.

$\text{CeT}_2\text{Si}_2$  ( $T$ : transition metal element) crystallizes in a  $\text{ThCr}_2\text{Si}_2$ -type tetragonal structure. These compounds have been well known to show many interesting electronic properties such as magnetic ordering, superconductivity, and so forth.<sup>3</sup> These anomalous properties are considered to be due to electronic and magnetic instability of  $4f$  electron state since several kinds of interactions such as the Ruderman-Kittel-Kasuya-Yosida (RKKY) interaction, the Kondo effect, and crystalline electric field are competing with each other in these compounds. Recently, a superconducting transition has

been found in several compounds under hydrostatic pressure near a QCP just at the border of magnetism where  $T_N \rightarrow 0$ , notably in  $\text{CeCu}_2\text{Ge}_2$ ,<sup>4</sup>  $\text{CePd}_2\text{Si}_2$ ,<sup>5</sup> and  $\text{CeRh}_2\text{Si}_2$ .<sup>6</sup> All these systems show antiferromagnetic ordering at ambient pressure.

$\text{CeRh}_2\text{Si}_2$  is also an antiferromagnet at ambient pressure. It has been revealed by neutron diffraction that the Bragg reflection represents the magnetic modulation with the wave vector of  $\mathbf{q}_1 = (0.5, 0.5, 0)$  below  $T_{N1} = 36$  K, where the magnetic moments are arranged along the  $c$  axis. Furthermore, the second Bragg reflection due to the wave vector of  $\mathbf{q}_2 = (0.5, 0.5, 0.5)$  starts growing at  $T_{N2} = 24$  K.<sup>7</sup>

It has been reported that the resistivity and the thermal expansion show anomalies near  $T_{N1}$  and  $T_{N2}$ .<sup>8,9</sup>  $T_{N1}$  and  $T_{N2}$  are suppressed by applying pressure and disappear near the critical pressure at  $P_{C1} \sim 1.0$  GPa and  $P_{C2} \sim 0.6$  GPa, respectively. It implies that there are two phase transitions at zero temperature, that is, QPT, one of which,  $P_{C1}$ , separates magnetic ordering phase with the wave vector of  $\mathbf{q}_1$  from the one with no long range order, and the other,  $P_{C2}$ , separates two magnetic phases. The superconductivity appears at 400 mK at 0.9 GPa, near the critical pressure  $P_{C1}$  required to completely suppress antiferromagnetic ordering.<sup>6</sup>

In the present work, we report the electrical resistivity and x-ray diffraction under pressure in detail and discuss the electronic properties of a single crystalline  $\text{CeRh}_2\text{Si}_2$  near the pressure-induced QCP. The electrical resistivity of a FL exhibits a contribution  $\rho(T) = \rho(0) + AT^2$  at low temperature, where  $A$  is usually attributed to the Umklapp process of the electron-electron collisions. However, in the vicinity of the magnetic-nonmagnetic transition, non-fermi-liquid (NFL) behaviors are often observed as a strong deviation of transport properties from FL predictions, which is indicated as a power law such as  $\rho(T) = \rho(0) + AT^m$ ,  $m < 2$ . Even if

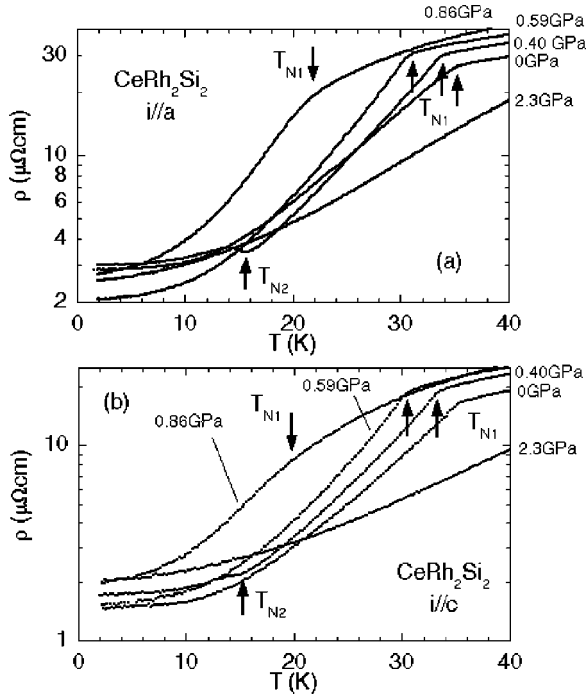


FIG. 1. Temperature dependence of the electrical resistivity of  $\text{CeRh}_2\text{Si}_2$  along the (a)  $a$  and (b)  $c$  axes.

such behaviors are not observed, some crossover from NFL to FL may be found near QCP. In this paper, we discuss the electronic properties and the FL instability near QPT induced by pressure.

## II. EXPERIMENTAL

Single crystal of  $\text{CeRh}_2\text{Si}_2$  was grown by Czochralski pulling method in a tetra-arc furnace. The sample was annealed in a quartz tube under vacuum of  $1 \times 10^{-6}$  Torr at  $900^\circ\text{C}$  for one week. The electrical resistance for the current along both  $a$  and  $c$  axes was measured by the usual four-probe dc method, in which four gold leads were attached to the sample by means of silver paste. The residual resistivity ratio is 32 at ambient pressure. High pressure was generated up to 2.3 GPa by using a tungsten carbide piston and a Ni-Cr-Mo-Co alloy (MP35N) cylinder.<sup>10</sup> The pressure was always kept constant in the temperature range between 2 and 300 K by controlling the load within  $\pm 1\%$ . A mixture of Fluorinerts of FC70 and FC77 in ratio 1:1 was used as a pressure transmitting medium. Above 2.3 GPa, the electrical resistance was measured for the current along the  $a$  axis by using a cubic anvil-type high-pressure cell up to 8 GPa.<sup>11</sup>

The pressure dependence of lattice parameters was determined by x-ray ( $\text{MoK}\alpha$ ) powder diffraction with a Guinier-type focusing camera and highly sensitive film. Hydrostatic pressure was generated by using tungsten-carbide Bridgman anvils and a Be sheet as a gasket. Details of the pressure apparatus have been reported previously.<sup>12</sup>

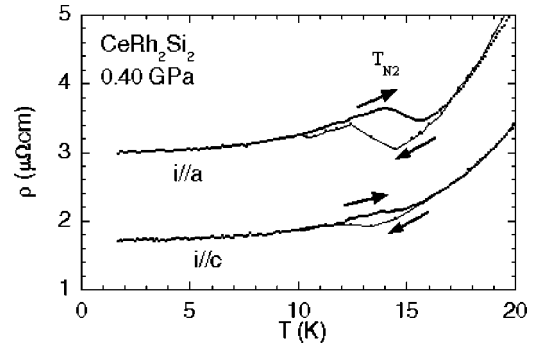


FIG. 2. The electrical resistivity at 0.4 GPa below 20 K.

## III. RESULTS AND DISCUSSION

### A. Disappearance of antiferromagnetism at high pressure below 2 GPa

Figure 1 shows the electrical resistivity  $\rho(T)$  for the  $a$  and  $c$  axes as a function of temperature below 40 K under high pressures. At ambient pressure, the resistivity shows a sudden decrease near 35 K ( $=T_{N1}$ ) and a small anomaly near 24 K ( $=T_{N2}$ ). The anomalies at  $T_{N1}$  and  $T_{N2}$  correspond to the magnetic phase transitions which were mentioned before. The anomaly near  $T_{N1}$  becomes less prominent with increasing pressure, corresponding to the pressure-induced decrease of the sublattice magnetization.<sup>7</sup>  $T_{N1}$  decreases with increasing pressure and disappears above 1.0 GPa ( $\sim P_{C1}$ ).

$T_{N2}$  also decreases with increasing pressure and disappears above 0.58 GPa ( $\sim P_{C2}$ ). At 0.4 GPa, on the other hand, it is found that  $\rho(T)$  shows a minimum  $T_{N2} \sim 14.5$  K along the  $a$  and  $c$  axes. Furthermore, as seen in Fig. 2, the hysteresis is found near  $T_{N2}$  along the  $a$  and  $c$  axes, indicating that this transition is first order. Although no hysteresis in the  $\rho(T)$  curve is observed at ambient pressure, the results of strain measurements on a single crystal of  $\text{CeRh}_2\text{Si}_2$  show a discontinuity in the length of the  $a$  and  $c$  axes<sup>13</sup> which is consistent with a first-order transition near 26 K. The discontinuous change at  $T_{N2}$  increases with increasing pressure,<sup>14</sup> corresponding to the enhancement of the anomaly on  $\rho(T)$  curve near  $T_{N2}$  by applying pressure.

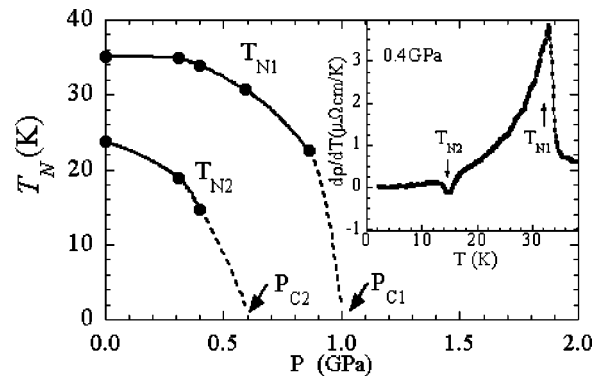


FIG. 3. Pressure dependence of the critical temperatures  $T_{N1}$  and  $T_{N2}$  of  $\text{CeRh}_2\text{Si}_2$ . Broken lines are extrapolations. An example of the  $d\rho/dT$  at 0.4 GPa is shown in the inset.

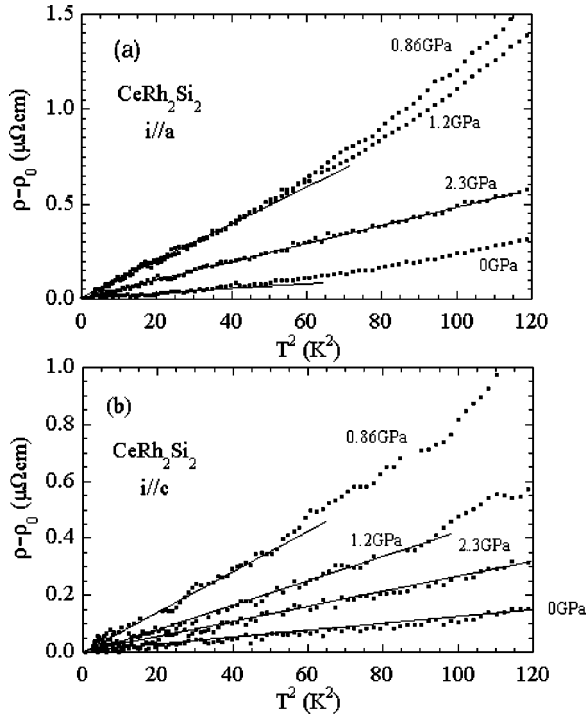


FIG. 4.  $T^2$  dependence of  $\Delta\rho = \rho - \rho_0$  of CeRh<sub>2</sub>Si<sub>2</sub> along (a)  $a$  and (b)  $c$  axes.

The pressure dependence of  $T_{N1}$  and  $T_{N2}$  is plotted in Fig. 3. The magnetic phase transition temperatures  $T_{N1}$  and  $T_{N2}$  were determined by calculating the temperature derivatives of  $\rho(T)$ ,  $d\rho/dT$ , which is shown in the inset of Fig. 3. It is in good agreement with that determined by the measurement of thermal expansion.<sup>8</sup> We have found that the transition at  $T_{N1}$  is second order and that at  $T_{N2}$ , first order.  $T_{N1}$  decreases gradually at low pressure and then abruptly near 1 GPa, which is the critical pressure  $P_{C1}$  where the transition disappears. Qualitatively, the phase boundary of  $T_{N1}(P)$  is interpreted on the basis of Doniach's model for competing Kondo and RKKY interactions.<sup>15</sup>

In CeRh<sub>2</sub>Si<sub>2</sub>, the magnetic order is present because the RKKY interaction overcomes the Kondo effect at low temperature. By considering that  $T_{N1}$  decreases with pressure, CeRh<sub>2</sub>Si<sub>2</sub> is on the right hand side of Doniach's phase diagram. The antiferromagnetic order is destroyed by increasing the coupling constant  $JN(0)$ , which means an increase of pressure. The ground state then becomes a FL with a rather large effective mass for the fermionic quasiparticles, indicating a large spin fluctuation near pressure-induced quantum phase transition, which will be discussed later.

Next, we discuss briefly the thermodynamic property on the slope of the phase boundary at  $T_{N2}$ . At ambient pressure, the discontinuity of the entropy  $\Delta S$  is estimated to be 0.06 J/mol K.<sup>13</sup>  $\Delta V$  is obtained from the discontinuity of the thermal expansion,  $\Delta V/V = -6 \times 10^{-5}$  (Ref. 13) and  $V = 4.8 \times 10^{-5} \text{ m}^3/\text{mol}$  is taken from the lattice parameter. By using the Clausius-Clapeyron relation,  $\partial T_{N2}/\partial P = \Delta V/\Delta S \sim 0$ . Although the discontinuity of the volume  $\Delta V$  is almost independent of pressure,<sup>8,14</sup> the slope of  $\partial T_{N2}/\partial P$  becomes

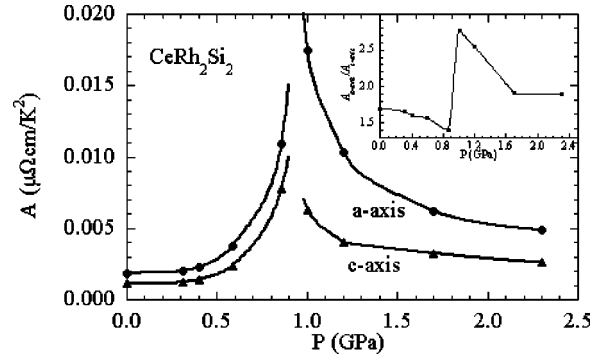


FIG. 5. Pressure dependence of the coefficient of  $T^2$  of CeRh<sub>2</sub>Si<sub>2</sub> along the  $a$  and  $c$  axes. The inset shows the ratio  $A_a/A_c$  as a function of pressure.

steep as pressure increases. It is suggested that  $\Delta S$  is suppressed by applying pressure below  $P_{C2}$ .

The resistivity  $\rho$  is described as  $\rho = \rho_0 + AT^2$  at low temperature in a wide pressure range, where  $\rho_0$  is the residual resistivity and  $A$  the constant. Figure 4 shows the  $T^2$  dependence below 2.3 GPa along the  $a$  and  $c$  axes. In the case of the present work, the  $T^2$  term of  $\rho$  is attributed to the effect of spin fluctuation or the contribution from electron-magnon scattering.

The values of  $A$  for the  $a$  and  $c$  axes,  $A_a$  and  $A_c$ , are shown in Fig. 5 as a function of pressure. Broken curves are a guide to the eyes. If the  $T^2$  term of  $\rho$  is mainly attributed to the electron-magnon scattering, the value of  $A(P)$  should decrease up to  $P_{C1} \sim 1.0$  GPa where magnetic ordering disappears. However, it is found that both  $A_a(P)$  and  $A_c(P)$  show maxima near 1.0 GPa, where the effect of spin fluctuation is expected to be most significant. It means that the large enhancement in the  $T^2$  term is not due to the electron-magnon scattering but due to the existence of large spin fluctuation around the critical pressure  $P_{C1}$ , which corresponds to the pressure-induced quantum phase transition. Qualitatively, the pressure dependence of  $A(P)$  is consistent with that of Sommerfeld coefficient  $\gamma$  of specific heat,<sup>16</sup> in which  $\gamma(P)$  increases from 20 mJ/mol K<sup>2</sup> at ambient pressure and passes through a broad maximum of 80 mJ/mol K<sup>2</sup> near 1.0 GPa. On the other hand, no anomaly is observed near  $P_{C2}$ . Since this transition is first order, no fluctuation may exist and therefore the coefficient  $A$  is not affected.

It is noted that the value of  $A$  shows large anisotropy between the  $a$  and  $c$  axes. The inset in Fig. 5 shows the pressure dependence of the ratio  $A_a/A_c$ . A discontinuity is observed at the critical pressure near  $P_{C1}$  and a small anomaly near  $P_{C2}$ . The resistivity is usually calculated from the displacement of the Fermi surface by an electric field. When the Fermi surface is anisotropic, the resistivity depends on the direction of the current density in the crystal. If the values of  $A_a$  and  $A_c$  come from the umklapp process of the electron-electron collisions, they may be related to the area (or cross section) of Fermi surfaces that have been sliced perpendicular to the  $a$  and  $c$  directions in  $k$  space. Because several scattering mechanisms are included in the

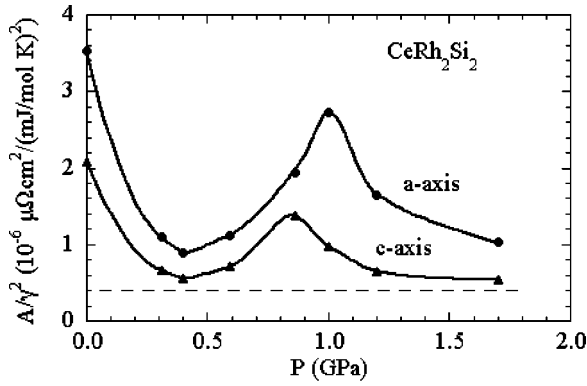


FIG. 6. Pressure dependence of the ratio of  $A/\gamma^2$  of  $\text{CeRh}_2\text{Si}_2$  along the  $a$  and  $c$  axes.

electrical resistivity, it is suggested that this transition corresponds a change in the topology of the Fermi surface at high pressure.

In general, the coefficient  $A$  of  $T^2$  term in the resistivity and the linear specific heat coefficient  $\gamma$  appear to have the so-called Kadowaki-Woods relation  $A \propto \gamma^2$ .<sup>17,18</sup> If the effective mass of conduction electron is essentially determined by the properties of a conventional band without a many body effect, such as in ordinary transition metals, the ratio  $A/\gamma^2 \sim 0.4 \times 10^{-6}$  is expected. In the case for HF compounds, on the other hand, the heavy mass is essentially due to the many-body dynamical effect between the lattice of local moments and the conduction electrons. It should be noted that for the system with many-body correlations, the ratio  $A/\gamma^2$  must have the value larger than that of transition metals.

In order to investigate the many-body electron correlation near QPT, the value of  $A/\gamma^2$  is plotted in Fig. 6 as a function of pressure. The value of  $\gamma$  is taken from the result of specific heat under pressure.<sup>16</sup> The ratio  $A/\gamma^2$  is found to depend on pressure since the behavior of  $A(P)$  is different quantitatively from that of  $\gamma(P)$ . The dashed line means the universal value  $A/\gamma^2 \sim 0.4 \times 10^{-6}$  which the ordinary transition metals make.<sup>18</sup> At ambient pressure, both  $A_a/\gamma^2$  and  $A_c/\gamma^2$  are much larger than those of transition metals. This indicates that the effect of magnetic fluctuation is included in both  $A$  and  $\gamma$  values. At low pressures below 0.4 GPa,  $A/\gamma^2$  decreases rapidly, which is a result of the vanishing of magnetic order. Above 0.6 GPa, however,  $A/\gamma^2$  is found to increase strongly with pressure below 0.9 GPa. Moreover, it decreases again with pressures up to 1.7 GPa, the value of which,  $A_a/\gamma^2 \sim 1.0 \times 10^{-6}$  and  $A_c/\gamma^2 \sim 0.5 \times 10^{-6}$  at 1.7 GPa, is almost the same as that of transition metals. This indicates that the large fluctuation is induced at the critical pressure  $P_{C1}$ , and a crossover from HF state to intermediate valence state occurs at high pressure.

Such behavior has been observed in a ferromagnet  $\text{UGe}_2$ .<sup>19,20,22</sup> It shows ferromagnetic ordering at  $T_C = 52$  K at ambient pressure.  $T_C$  and  $T^*$ , which are characteristic transition temperatures observed below  $T_C$ , decrease with increasing pressure and become zero around 1.9 and 1.2 GPa. At low pressures below 1 GPa, the value of  $A/\gamma^2 \sim 1 \times 10^{-5}$  is near the empirical universal value for HF systems. Up to 1.1 GPa,  $A/\gamma^2$  decreases to  $3.3 \times 10^{-6}$ , where the

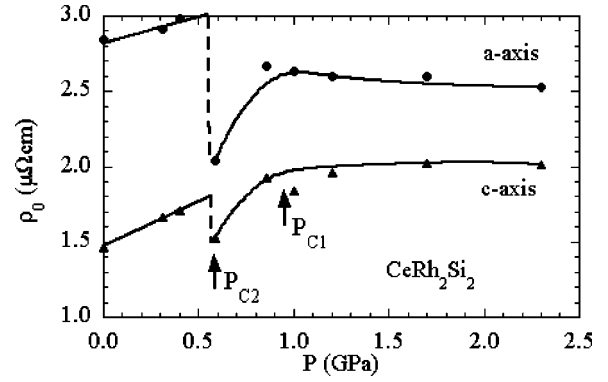


FIG. 7. Pressure dependence of the residual resistivity  $\rho_0$  of  $\text{CeRh}_2\text{Si}_2$  along the  $a$  and  $c$  axes.

transition characterized by  $T^*$  disappears. Moreover it increases significantly again to  $9 \times 10^{-6}$  around 1.3 GPa, where the value of  $A(P)$  shows a peak. This result implies that the peak in the  $A/\gamma^2$  vs  $P$  curve is closely related to the occurrence of the superconductivity in these materials.

Next, the values of the residual resistivity  $\rho_0(P)$  for the  $a$  and  $c$  axes are shown in Fig. 7 as a function of pressure. Solid curves are guides to the eyes. As for both the  $a$  and  $c$  axes,  $\rho_0(P)$  increases slightly as pressure increases, and decreases with a minimum near 0.6 GPa  $\sim P_{C2}$ , where the magnetic phase transition disappears ( $T_{N2} = 0$ ). The result indicates that the critical point near  $P_{C2}$  affects the magnitude of  $\rho_0$ . The discontinuous change of  $\rho_0$  at  $P_{C1}$  along the  $a$  axis is larger than that along the  $c$  axes.

It is difficult to show whether an anomaly on  $\rho_0(P)$  exists near  $P_{C1}$ . In the case of a ferromagnetic QCP, the anomaly of  $\rho_0$  is expected to be observed at the critical point, while the less pronounced anomalies expected in the case of AF-QCP.<sup>21</sup> In the case of  $\text{CeRh}_2\text{Si}_2$ , on the other hand, the resistivity exhibits a  $T^2$  dependence at low temperature having the large coefficient  $A(P)$  near  $P_{C1}$ . The value of  $A$  is

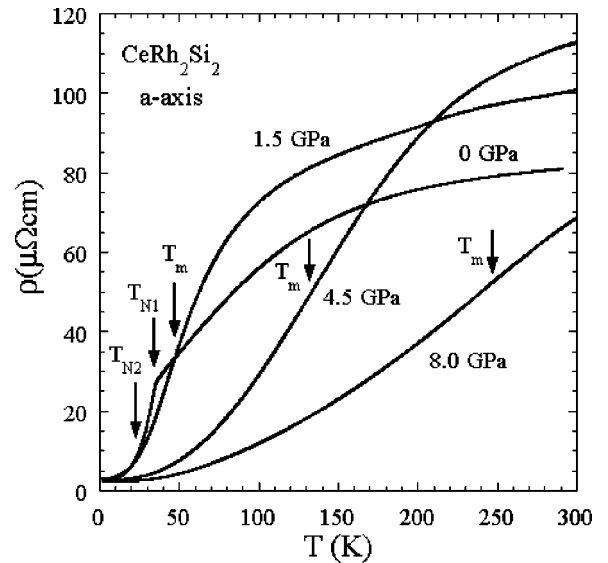
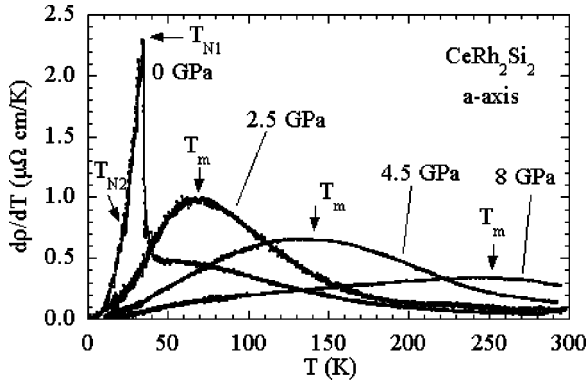


FIG. 8. Temperature dependence of the electrical resistivity of  $\text{CeRh}_2\text{Si}_2$  along the  $a$  axis up to 8 GPa.

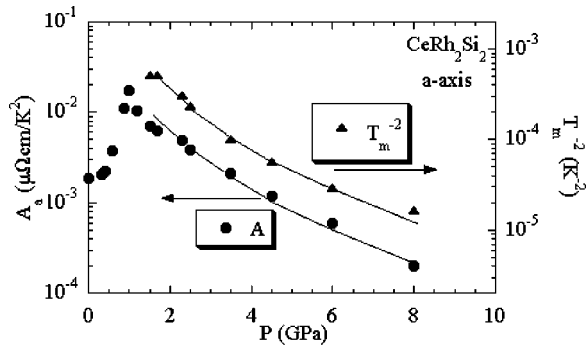
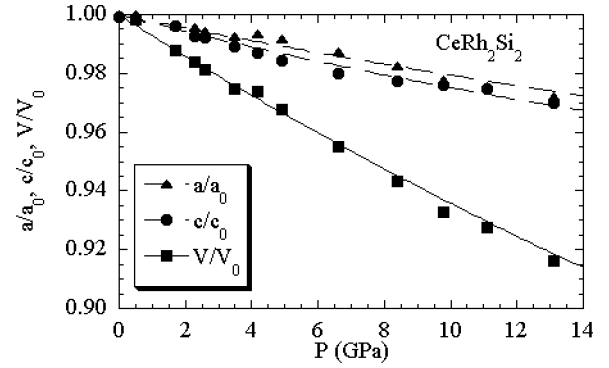

 FIG. 9. Temperature derivative  $d\rho/dT$  of CeRh<sub>2</sub>Si<sub>2</sub> up to 8 GPa.

usually attributed to the Umklapp process, which is related to the magnitude of spin fluctuation in the present work. Although, it is observed that  $\rho_{4.2\text{ K}}$  shows a peak at  $P_{C1}$  in the polycrystalline sample,<sup>22</sup> it may come from the large value of the  $AT^2$  term contributes to  $\rho(P)$  at 4.2 K and then  $\rho(P)$  may also show a maximum even when it shows no anomaly at  $T \rightarrow 0$  K.

### B. Kondo scattering above 2 GPa

Figure 8 shows the temperature dependence of the electrical resistivity in a wide temperature range under high pressures up to 8 GPa. No anomaly was detected in the  $\rho(T)$  above 1.5 GPa since magnetic orderings were suppressed completely. Instead, an inflection point at  $T_m$  is observed in the  $\rho(T)$  curve above 1.5 GPa.  $T_m$  is found to shift rapidly from 44 K at 1.5 GPa to higher temperature with increasing pressure. To show the results more clearly, the temperature derivative of  $\rho(T)$  curve was calculated. The values of  $d\rho/dT$  are shown in Fig. 9 as a function of  $T$ . A peak is clearly seen above  $P_{C1}$ .  $T_m$ , which is defined as the temperature showing the peak, increases with increasing pressure.

$T^2$  dependence was observed at low temperature below  $T_m$ . The coefficients  $A_a$  decrease significantly with increasing pressure: the value of  $A_a$  at 8 GPa is smaller than that at 1.5 GPa by two orders of magnitude. Figure 10 shows the pressure dependence of the values of  $A_a$  and  $T_m^{-2}$  up to 8 GPa. It

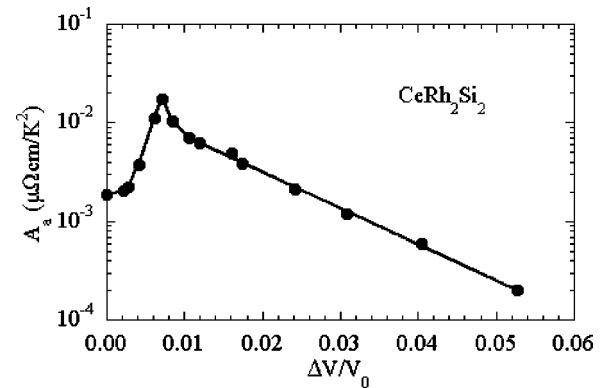

 FIG. 10.  $A_a$  and  $T_m^{-2}$  as a function of pressure. Two solid lines are guides to eye to show that the curve of  $A$  vs  $P$  is the same as that of  $T_m^{-2}$  vs  $P$ .

 FIG. 11. Pressure dependence of  $a/a_0$ ,  $c/c_0$ , and  $V/V_0$  of CeRh<sub>2</sub>Si<sub>2</sub>. The solid line for the pressure dependence of  $V/V_0$  shows the result of the least square fitting of Murnaghan's equation. The dashed lines for  $a/a_0$  and  $c/c_0$  are guides to the eye.

is found that the pressure vs  $A$  curve is proportional to that for  $T_m^{-2}$ , i.e.,  $A$  is approximately proportional to  $T_m^{-2}$  above  $P_{C1}$ . According to the theory of Yoshimori and Kasai,<sup>23</sup> the value of  $A$  is proportional to  $T_K^{-2}$ . It has been confirmed that the relation  $A \propto T_m^{-2}$  is valid in the heavy fermion materials.<sup>24</sup> These facts indicate that  $T_m$  is proportional to a characteristic temperature or Kondo temperature  $T_K$ ,  $T_m \propto T_K$ .

$T_K$  is also estimated from the temperature where magnetic susceptibility shows the peak. At ambient pressure,  $T_K$  is obtained to be  $\sim 35$  K and increases with pressure.<sup>25</sup> The slope of  $dT_K/dP$  is calculated to be 0.046 K/GPa from the result up to 1 GPa, while the large value  $dT_m/dP > 15$  K/GPa above 1.5 GPa is obtained in the present work. It is considered that below  $P_{C1}$ , two kinds of interactions, the RKKY interaction and the Kondo effect, are competing with each other and  $T_K$  is related not only to the Kondo effect but also to the RKKY interaction. Above  $P_{C1}$ , where the antiferromagnetic interaction disappears,  $T_K$  is expected to become sensitive with pressure as typical heavy fermion compounds.

### C. X-ray diffraction at high pressure

In order to investigate pressure dependence of lattice parameters, x-ray diffraction measurements were carried out.


 FIG. 12.  $A_a$  as a function of fractional change in volume  $\Delta V/V_0$ .

At ambient pressure, the crystal structure is tetragonal having the lattice parameters of  $a=4.070 \text{ \AA}$  and  $c=10.156 \text{ \AA}$ , which are consistent with previous experiments.<sup>13</sup> The lattice constants are determined mainly from the reflections (101), (103), and (112). Figure 11 shows the pressure dependences of the relative lattice parameters  $a/a_0, c/c_0$  and the relative volume  $V/V_0$  as a function of pressure at room temperature, where  $a_0, c_0,$  and  $V_0$  are the values at ambient pressure. It was revealed that the tetragonal structure is stable up to 13 GPa at room temperature. Both  $a$  and  $c$  decrease with increasing pressure, and no discontinuous change is observed within the experimental errors. The  $c$  axis is more compressible than the  $a$  axis, and linear compressibilities  $\kappa_i = -i^{-1} \partial i / \partial P$ ,  $i=a$  or  $c$ , are estimated to be  $2.2 \times 10^{-3}$  and  $3.0 \times 10^{-3} \text{ GPa}^{-1}$ .

We attempted a least-squares fit of the data of  $V/V_0$  to the first-order Murnaghan's equation of state  $P=(B_0/B'_0) \times [(V_0/V)^{B'_0} - 1]$ , where  $B_0$  denotes the bulk modulus at ambient pressure and  $B'_0$  is its pressure derivative. The results are shown in Fig. 11 as a solid curve for  $V/V_0$ . The agreement between the observed points and the calculated ones is satisfactory.  $B_0$  and  $B$  are estimated to be 139 and 2.2 GPa, respectively. The value of  $B_0$  of CeRh<sub>2</sub>Si<sub>2</sub> is comparable with those of typical heavy Fermion compounds such as CeCu<sub>6</sub> and CeInCu<sub>2</sub>.<sup>26</sup>

Here we estimate the Grüneisen parameter to evaluate the stability of electronic state above 2 GPa. The Grüneisen parameter  $\Gamma$  of  $T_K$  is written<sup>26</sup>

$$\Gamma = - \left. \frac{\partial \ln T_K}{\partial \ln V} \right|_{V=V_0} = \frac{1}{2} \left. \frac{\partial \ln A}{\partial \ln V} \right|_{V=V_0} = \frac{1}{2} \frac{\Delta(\ln A)}{\frac{\Delta V}{V_0}},$$

where  $A$  is the coefficient of  $T^2$  term. In Fig. 12, the values of  $A$  are plotted in logarithmic scale as a function of  $\Delta V/V_0$ .

The linear relationship is found in the plot as is shown by solid lines above 1.5 GPa ( $\Delta V/V_0 > 0.011$ ). From the result,  $\Gamma$  is estimated to be 42 for CeRh<sub>2</sub>Si<sub>2</sub>, which is extremely large and comparable with those of heavy fermion compounds 59 and 65 for CeInCu<sub>2</sub> and CeCu<sub>6</sub>, respectively.<sup>26</sup> Below 1.5 GPa, on the other hand, the observed values deviate significantly from the linear relation, suggesting a large enhancement of the Grüneisen parameter  $\Gamma$  near  $P_{C1}$ . This indicates that the electronic state is very unstable near  $P_{C1}$ .

#### IV. CONCLUSION

We have observed the electrical resistivity along the  $a$  and  $c$  axes of single crystalline CeRh<sub>2</sub>Si<sub>2</sub> under high pressure. As for the two magnetic-phase transitions, it has been found that the transition at  $T_{N1}$  is second order and at  $T_{N2}$ , first order. Temperature dependence of the resistivity shows  $T^2$  dependence at low temperature in a wide pressure range from ambient pressure up to 8 GPa, implying classical Fermi liquid behavior. The pressure dependence of the value of  $A/\gamma^2$ , however, suggests that the many-body dynamical effect is enhanced near the critical pressure  $P_{C1}$ . On the other hand, a discontinuous change near  $P_{C2}$  has been observed in the pressure dependence of the residual resistivity  $\rho_0(P)$ .

From the measurements of the electrical resistivity and lattice parameters of CeRh<sub>2</sub>Si<sub>2</sub> at high pressure, the volume dependence of Kondo temperature  $T_K$  was discussed. The Grüneisen parameter of  $T_K$  is estimated to be 42 above 1.5 GPa. The magnitude is comparable with those of heavy fermion compounds.

#### ACKNOWLEDGMENTS

This work was supported by a Grant in Aid for Scientific Research from the Japanese Ministry of Education, Science and Culture.

<sup>1</sup>S. Sachdev, *Quantum Phase Transitions* (Cambridge University Press, New York, 1999).

<sup>2</sup>H.v. Löhneysen, *J. Magn. Magn. Mater.* **200**, 532 (1999).

<sup>3</sup>A. Szytula and L. Leciejewicz, *Handbook on the Physics and Chemistry of Rare Earths*, edited by K.A. Gschneidner, Jr. and L. Eyring (1989), Vol. 12, pp. 133–211.

<sup>4</sup>D. Jaccard, K. Behnia, and J. Sierro, *Phys. Rev. Lett.* **163**, 475 (1992).

<sup>5</sup>N.D. Mathur, F.M. Grosche, S.R. Julian, I.R. Walker, D.M. Freye, R.K.W. Haseiwimmer, and G.G. Lomzarich, *Nature (London)* **394**, 39 (1998).

<sup>6</sup>R. Movshovich, T. Graf, D. Mandrus, J.D. Thompson, J.L. Smith, and Z. Fisk, *Phys. Rev. B* **53**, 8241 (1996).

<sup>7</sup>S. Kawarazaki, M. Sato, Y. Miyako, N. Chigusa, K. Watanabe, N. Metoki, Y. Koike, and M. Nishi, *Phys. Rev. B* **61**, 4167 (2000).

<sup>8</sup>F. Honda, N. Matsuda, T. Kagayama, G. Oomi, Y. Ōnuki, and E.V. Sampathkumaran, *J. Magn. Soc. Jpn.* **23**, 474 (1999).

<sup>9</sup>M. Ohashi, S. Kaji, I. Minamitake, F. Honda, T. Eto, G. Oomi, S. Koivai, and Y. Uwatoko, *Physica B* **312–313**, 443 (2002).

<sup>10</sup>F. Honda, S. Kaji, I. Minamitake, M. Ohashi, G. Oomi, T. Eto, and T. Kagayama, *J. Phys.: Condens. Matter* **14**, 11 501 (2002).

<sup>11</sup>N. Mōri, Y. Okayama, H. Takahashi, Y. Haga, and T. Suzuki, *Jpn. J. Appl. Phys.* **8**, 182 (1993).

<sup>12</sup>T. Kagayama and G. Oomi, *J. Magn. Magn. Mater.* **140–144**, 1227 (1995).

<sup>13</sup>R. Settai, A. Misawa, S. Araki, M. Kosaki, K. Sugiyama, T. Takeuchi, K. Kindo, Y. Haga, E. Yamamoto, and Y. Ōnuki, *J. Phys. Soc. Jpn.* **66**, 2260 (1997).

<sup>14</sup>T. Kagayama (private communication).

<sup>15</sup>S. Doniach, in *Valence Instabilities and Related Narrow Band Phenomena*, edited by R.D. Parks (Plenum, New York, 1977), p. 169.

<sup>16</sup>T. Graf, J.D. Thompson, M.F. Hundley, R. Movshovich, Z. Fisk, D. Mandrus, R.A. Fisher, and N.E. Phillips, *Phys. Rev. Lett.* **78**, 3769 (1997).

<sup>17</sup>K. Kadowaki and S.B. Woods, *Solid State Commun.* **58**, 507 (1986).

<sup>18</sup>K. Miyake, T. Matsuura, and C.M. Varma, *Solid State Commun.* **71**, 1149 (1989).

- <sup>19</sup>N. Tateiwa, T.C. Kobayashi, K. Hanazono, K. Amaya, Y. Haga, R. Settai, and Y. Onuki, *J. Phys.: Condens. Matter* **13**, L17 (2001).
- <sup>20</sup>G. Oomi, T. Kagayama, and Y. Ōnuki, *J. Alloys Compd.* **271–273**, 482 (1998).
- <sup>21</sup>K. Miyake and O. Narikiyo, *J. Phys. Soc. Jpn.* **71**, 867 (2002).
- <sup>22</sup>G. Oomi, T. Kagayama, F. Honda, Y. Ōnuki, and E.V. Sampathkumaran, *Physica B* **281&282**, 393 (2000).
- <sup>23</sup>A. Yoshimori and H. Kasai, *J. Magn. Magn. Mater.* **475**, 31 (1983).
- <sup>24</sup>T. Kagayama, G. Oomi, H. Takahashi, N. Mōri, Y. Ōnuki, and T. Komatsubara, *Phys. Rev. B* **44**, 7690 (1991).
- <sup>25</sup>H. Mori, N. Takeshita, N. Mōri, and Y. Uwatoko, *Physica B* **259–261**, 58 (1999).
- <sup>26</sup>T. Kagayama and G. Oomi, *J. Phys. Soc. Jpn.* **65**, 42 (1996).